https://doi.org/10.1016/j.ijheatmasstransfer.2023.124666

Elucidating the automobile proton exchange membrane fuel cell of innovative double-cell structure by full-morphology simulation

Lizhen Wu[a], Guobin Zhang[b, *], Biao Xie[c], Wenming Huo[c], Kui Jiao[c, d, *], Liang An[a, *]

a. Department of Mechanical Engineering, The Hong Kong Polytechnic University, Hung Hom, Kowloon, Hong Kong Special Administrative Region, China

b. MOE Key Laboratory of Thermo-Fluid Science and Engineering, School of Energy and Power Engineering, Xi'an Jiaotong University, Xi'an 710049, China

c. State Key Laboratory of Engines, Tianjin University, 135 Yaguan Rd, Tianjin 300350, China

d. National Industry-Education Platform of Energy Storage, Tianjin University, 135 Yaguan Rd, Tianjin, China, 300350

*Corresponding author. E-mail: zhangguobin@xjtu.edu.cn (G. Zhang); kjiao@tju.edu.cn (K. Jiao); liang.an@polyu.edu.hk (L. An)

Abstract

The structural design of PEM fuel cell is crucial to improving its power density, and the cell structure largely depends on the bipolar plate (BP). This study compares the conventional single-cell structure and double-cell structure through three-dimensional (3D) large-scale (cell area: 312 cm^2) full-morphology simulation. As for the double-cell structure, the channels are arranged in a dislocation manner and there is one cooling flow field per two cells. For the structure of the BP, we also fully considered the realistic morphology of distribution area and the coolant flow. It is found that the heat dissipation effect of double-cell structure is worse but the performance is very close compared to single-cell structure. Moreover, its volumetric power density is significantly improved (~ 20%) due to the reduction in height. It is also found that increasing the velocity of coolant in the double-cell structure increases the performance first and then decreases.

Keywords: PEM fuel cell; double-cell structure; full-morphology simulation; power density; coolant flow.

1. Introduction

Currently, the application of proton exchange membrane (PEM) fuel cell in automobiles, i.e. fuel cell vehicles (FCVs) [1, 2], is receiving worldwide attention due

to the advantages of high efficiency, high power density, and zero emission, etc. [3-5]. However, it is still in the early commercial stage and the power density of PEM fuel cells must be increased from state-of-the-art 4.4 to 9.0 kW L^{-1} before industrial application [6-7], which means higher output power and lower cell/stack volume/weight. To achieve this target, in addition to the development of high-performance membrane electrode assembly (MEA), it is also of significant importance to design a proper cell structure decreasing the cell thickness/volume without decreasing the cell performance [8].

In general, the bipolar plates (BPs) account for about 70–90% of the cell/stack volume/weight, and hence it plays a determinative role in the cell thickness/volume reduction [9]. In recent years, Honda proposed an innovative double-cell structure with 1 cooling plate per 2 cells (Figure 1) and implemented in the Clarity FCV successfully, which significantly decreases the average cell thickness to about 1.0 mm, about 20% lower than the industry average level [8]. However, as far as authors know, the influences of this cell structure on the water and thermal state inside the cell and the cell performance have not been reported in the open literature. In this study, the full-scale 3D multiphase simulation is conducted on the automobile PEM fuel cells of conventional single-cell and innovative double-cell structures, in which the full BP morphology with the distribution zones for hydrogen, air and coolant is also considered (Figure 1).

2. Methods

2.1 Computational domain

Figure 1 shows the computational domain of automobile PEM fuel cell used in this study, which includes metallic bipolar plates (BPs), gas diffusion layers (GDLs), microporous layers (MPLs), catalyst layers (CLs) and PEM. The MEA area is 312 cm^2, and there are 80 parallel channels in both anode and cathode BPs. The research focus of this study is still on the comparison of the structural features of the stack. Therefore, whether it is single-cell or double-cell, it can be accepted when ensuring that the main region is the same.

The distribution zones guiding the hydrogen, air and coolant flow are assigned at

two sides of the flow channels, in which the square dots are interspersed in order to improve the uniformity of fluid flow into each channel as much as possible [10]. For simplicity, only the void parts for fluid flow in the distribution zones are included in the computational domain. The flow directions of hydrogen and that of air and coolant are opposite. In fact, this is also the most popular cell structure in FCVs [11-13], and the detailed geometry parameters can be found in Figure 1 and Table S1. In comparison with the conventional single-cell structure, the double-cell structure eliminates the coolant plate between two adjacent cells, and decreases the thickness of a flow channel (0.177 mm in this case study) every two cells, as shown in Figure 1. In this case study, the cell thicknesses of single-cell and double-cell structures are 0.996 and 0.819 mm (the thicknesses of double-cell stack is 1.638 mm and each cell is 0.819 mm), respectively.

2.2 Governing equations

The three-dimensional (3D) PEM fuel cell model used in this study is developed by adding the governing equations describing the coolant flow in our previous model [14]. The detailed governing equations are listed in Supplemental file.

2.3 Boundary conditions

At the anode and cathode channel inlets, the mass flow rates are specified [15], and the velocity is specified at the cooling channel inlets. Correspondingly, the constant pressures are specified at the gas and cooling channel outlets. Meanwhile, considering that almost all the waste heat produced in the PEM fuel cell is blown away by the coolant flow, all the surrounding surfaces of the computational domain are set to be adiabatic, i.e. zero heat flux [16]. In addition, the operating current density and reference voltage (0 V) are specified at the outer surfaces of anode and cathode BPs, respectively. As for the double-cell structure, the operating current density is specified at the outer surface of anode BP in Cell 1, and the reference voltage (0 V) is specified at the outer surface of cathode BP in Cell 2.

2.5 Numerical implementation

The 3D PEM fuel cell model adopted in this study is implemented in ANSYS

FLUENT, and the UDF (User Defined Function) code is incorporated in this model for customized governing equations, transport coefficients, source terms, boundary conditions, etc. In the computational domain, as shown in Figure 1, the distribution zones are meshed by tetrahedral grids and the other parts by hexahedral grids, and the Interface function in ANSYS FLUENT is activated to solve the mismatch issue at the interfaces between the distribution zones and flow fields. There are 11 and 24 million grid points in the PEM fuel cells of single-cell and double-cell structures, respectively. All simulation cases are performed on supercomputers and each case takes about 96 hours with 48 processors in parallel (CPU: AMD EPYC 7452 @ 2.35 GHz and 256G RAM).

3. Results and discussion

3.1 Cell performance characteristics

Figure 2 (a) shows the polarization curves and average temperatures at different current densities of PEM fuel cells with conventional single- and double-cell structures. Clearly, at the same coolant flow velocity, the average temperature of double-cell structure is a little higher, which is consistent with the temperature distributions shown in Figure 2 (c) and (d). This is mainly because the elimination of one cooling plate inside the two adjacent cells. However, its influence on the cell performance is negligible in this case study. The reason is that oxygen and water vapor concentration at CL have a competitive relationship under low humidity condition [7]. As shown in Figure 3 (c) and (d), it can be seen that higher temperature in double-cell will lead to higher water vapor concentration in CL compared with single-cell structure, which in turn affects membrane water hydration, proton conduction and increases ionic ohmic loss finally. In addition, the increase of water vapor concentration in the cathode CL will also dilute the oxygen and increase the concentration loss, but the effect is not obvious. On the other hand, higher temperature decreases the activation overpotential slightly. Therefore, the combined effects of concentration, ohmic and activation losses lead to little difference in output cell voltage between single-cell and double-cell structures especially at high current densities, as shown in Figure 4. However, the average cell thickness is reduced by 17.7%, which contributes to the increase of power

density, as shown in Figure 2(b).

In addition, it can be seen in Figure 2 (c) and (d) that there are non-negligible differences in the current density distribution between the two cells, but the differences in the temperature distribution are negligible. In fact, this is much likely to be caused by the dislocation of air flow channels in these two cells, as seen in Figure 3 (b), which induces the different distributions of oxygen and water vapor concentration (Figure 3 c and d). In fact, the cross flow under the rib between two adjacent channels in the GDL induced by the different pressures is helpful to mitigate this issue (Figure 3 b). But its influence is little in parallel straight channels. Considering that the different current density distributions may induce the durability concern in the practical applications, enhancing the cross flow between two adjacent channels by properly designing the flow field configuration, e.g. partially narrow channel adopted in 2nd-generation Mirai, alternately narrowed or baffled channel [17], etc.

3.2 Effect of coolant velocity

Considering that the poor cooling capacity of double-cell structure is likely to be avoided by increasing the coolant flow rate, we investigated the influence of coolant velocity at high current density (3.0 A cm^{-2}). The unexpected pumping power increase is evaluated by calculating the net power density [18]:

$$W_{\text{net}} = IV_{\text{out}} - \Delta P_{\text{cooling}} v_{\text{cooling}} A_{\text{cooling\_in}} / A_{\text{MEA}} / \zeta \qquad (1)$$

where v (m s^{-1}) the inlet average velocity, A_{in} (m^2) the inlet area, A_{MEA} (cm^2) the activation area and ζ the efficiency of the compressor (70% in the study [9]).

As shown in Figure 4, as the increase of the coolant velocity, the heat dissipation capacity of the PEM fuel cell is improved and the cell temperature is effectively reduced, which also slightly increases the cell voltage. However, the net power density will decrease when the coolant velocity is larger than 2 m s^{-1} in this case study due to the increase of pumping power, indicating that there is an optimal coolant flow rate satisfying the heat dissipation demand with low pumping power.

4. Conclusion

In this study, we numerically investigated the PEM fuel cell of an innovative

double-cell structure, in which there is one cooling unit every two cells, and compared it with conventional single-cell structure that has one cooling unit every one cell. The 3D modeling work is conducted a typical large-scale PEM fuel cell (cell area: 312 cm^2) used in FCV applications, and the realistic BP and cell morphology is included in detail. Specifically, the distribution zones with dot matrix dispersed for hydrogen, air and coolant flow next to the parallel channels are also included in the computational domain in order to be better consistent with the reality. It can be concluded from the simulation results that the double-cell structure has little influence on the cell power in all the current density regime, but it can increase the cell power density by about 20% benefitted from the average cell thickness reduction, in comparison with the conventional single-cell structure. However, this is at the expense of poorer heat dissipation capacity and different distributions of current density, oxygen concentration, water content, etc., between the two adjacent cells, which may impose the fuel cell to durability concern in long-term operation. For the poorer heat dissipation capacity, it is likely to be mitigated by properly increasing the coolant velocity. As for the non-uniform distribution, enhancing the cross flow between two adjacent channels by properly designing the flow field configuration is expected to make a difference.

Acknowledgements

This work was supported by the National Natural Science Foundation of China (No. 52206112), the Shenzhen Science and Technology Innovation Commission (No. SGDX2020110309520404), the Project funded by China Postdoctoral Science Foundation (No. 2022M710108), State Key Laboratory of Engines, Tianjin University (No. K2023-12), and the Fundamental Research Funds for the Central Universities (No. xzy012021018).

References

[1] Jiao K, Xuan J, Du Q, et al. Designing the next generation of proton-exchange membrane fuel cells. Nature, 2021, 595(7867): 361-369.

[2] Zhang G, Qu Z, Tao W Q, et al. Porous Flow Field for Next-Generation Proton Exchange Membrane Fuel Cells: Materials, Characterization, Design, and Challenges. Chemical Reviews, 2022, doi:

https://doi.org/10.1021/acs.chemrev.2c00539.

[3] Full Specs of Toyota MIRAI 2021. Toyota Motor Sales, U.S.A., Inc. (2020). https://www.toyota.com/MIRAI/features/mileage_estimates/3002/3003.

[4] Wang Y, Pang Y, Xu H, et al. PEM Fuel cell and electrolysis cell technologies and hydrogen infrastructure development: a review. Energy & Environmental Science, 2022.

[5] Cullen D A, Neyerlin K C, Ahluwalia R K, et al. New roads and challenges for fuel cells in heavy-duty transportation. Nature energy, 2021, 6(5): 462-474.

[6] Hydrogen, fuel cell project evaluation, and issue sharing week. Japan New Energy and Industrial Technology Development Organization (NEDO) Reports (2019). https://www.nedo.go.jp/events/report/ZZHY_00003.html.

[7] Suzuki,T. Challenges toward 2030/2040, https://www.nedo.go.jp/content/100888556.pdf.

[8] Zhang G, Wu L, Tongsh C, et al. Structure Design for Ultrahigh Power Density Proton Exchange Membrane Fuel Cell. Small Methods, 2023: 2201537.

[9] Wang, Y., Ruiz Diaz, D. F., et al. Materials, technological status, and fundamentals of PEM fuel cells – A review. Materials Today, 32, 2020: 178-203.

[10] Yong Z, Shirong H, Xiaohui J, et al. Characteristics of proton exchange membrane fuel cell considering “dot matrix” gas distribution zones and waveform staggered flow field with cooling channels. Energy Conversion and Management, 2022, 267: 115881.

[11] Zhang Y, Tao Y, Ren H, et al. A metallic gas diffusion layer and porous media flow field for proton exchange membrane fuel cells. Journal of Power Sources, 2022, 543:231847.

[12] Yu Y, Zhan Z, He L, et al. Effects of distribution zone design on flow uniformity and pressure drop in PEMFC. Journal of The Electrochemical Society, 2021, 168(9): 094505.

[13] Shen H, Huang Y, Kang H, et al. Effect of the cooling water flow direction on the performance of PEMFCs. International Journal of Heat and Mass Transfer, 2022, 189: 122303.

[14] Zhang G, Qu Z, Wang Y. Full-scale three-dimensional simulation of air-cooled proton exchange membrane fuel cell stack: Temperature spatial variation and comprehensive validation. Energy Conversion and Management, 2022, 270: 116211.

[15] Wang Y, Wang X, Qin Y, et al. Three-dimensional numerical study of a cathode gas diffusion layer with a through/in plane synergetic gradient porosity distribution for PEM fuel cells. International Journal of Heat and Mass Transfer, 2022, 188: 122661.

[16] Yong Z, Shirong H, Xiaohui J, et al. Characteristics of proton exchange membrane fuel cell considering “dot matrix” gas distribution zones and waveform staggered flow field with cooling channels. Energy Conversion and Management, 2022, 267: 115881.

[17] Qin Z, Huo W, Bao Z, et al. Alternating Flow Field Design Improves the Performance of Proton Exchange Membrane Fuel Cells. Advanced Science, 2022: 2205305.

[18] Zhang G, Fan L, Sun J, et al. A 3D model of PEMFC considering detailed multiphase flow and anisotropic transport properties. International Journal of Heat and Mass Transfer, 2017, 115: 714-724.

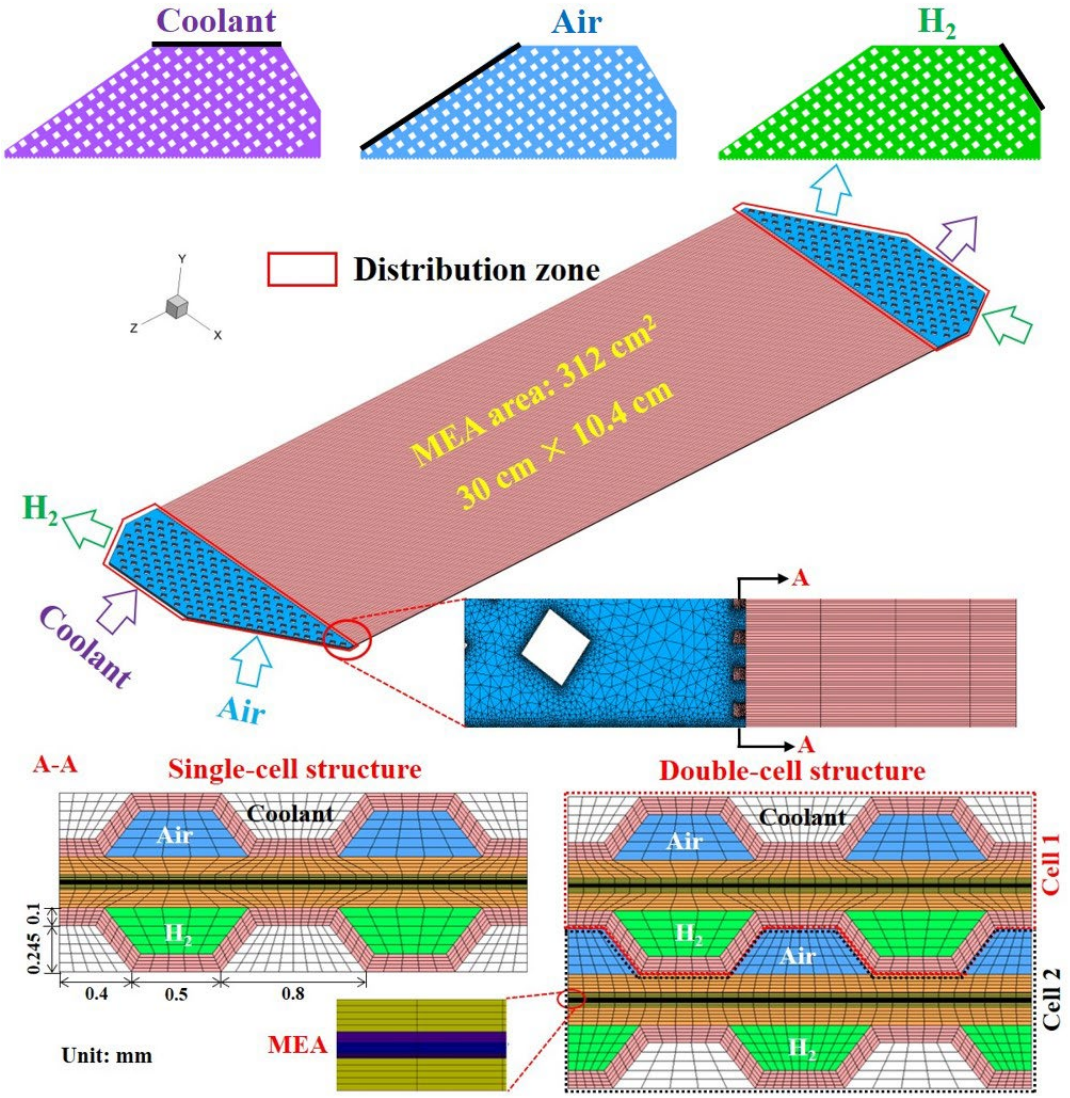

Figure 1. Computational domains of single-cell and double-cell structures

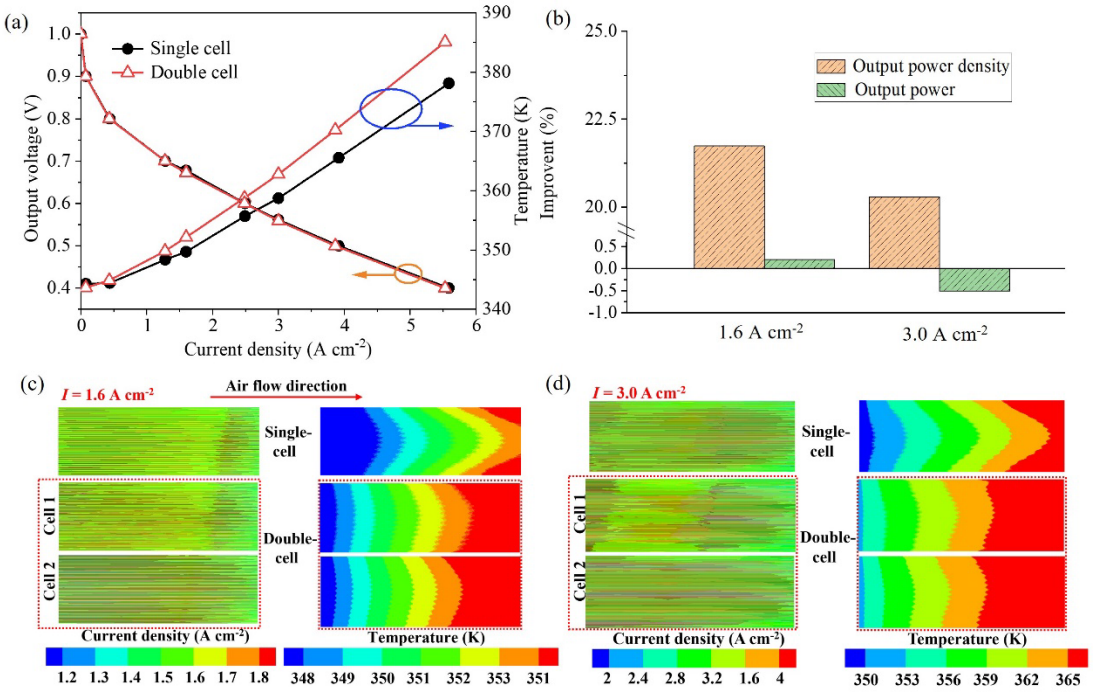

Figure 2. (a) Comparison of polarization curves and average temperature in the cathode CL of the single-cell and double-cell structure; (b) Output power and power density improvement of double-cell structure (single-cell structure as the base case); Current density distribution in the middle plane of the membrane, and temperature distribution in the middle plane of the cathode CL at (c) I =1.6 A cm^{-2}; (d) I = 3.0 A cm^{-2}.

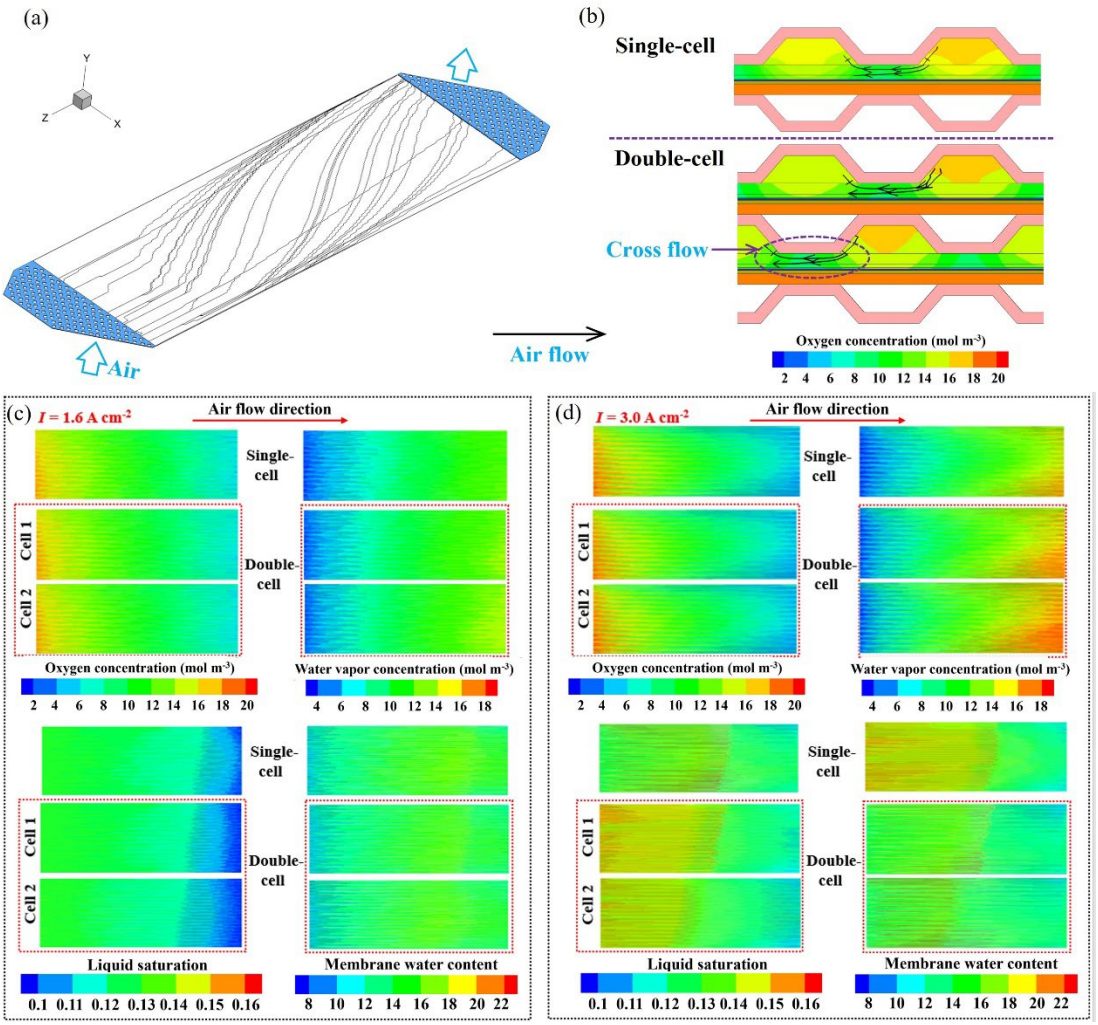

Figure 3. (a) Streamline in the middle plane (Y direction) of cathode channel; (b) Streamline and oxygen distribution in the middle plane (Z direction) of cathode channel; Oxygen concentration, water vapor concentration, liquid saturation and membrane water distribution in the middle plane of the cathode CL at (c) I =1.6 A cm^{-2}; (d) I = 3.0 A cm^{-2}.

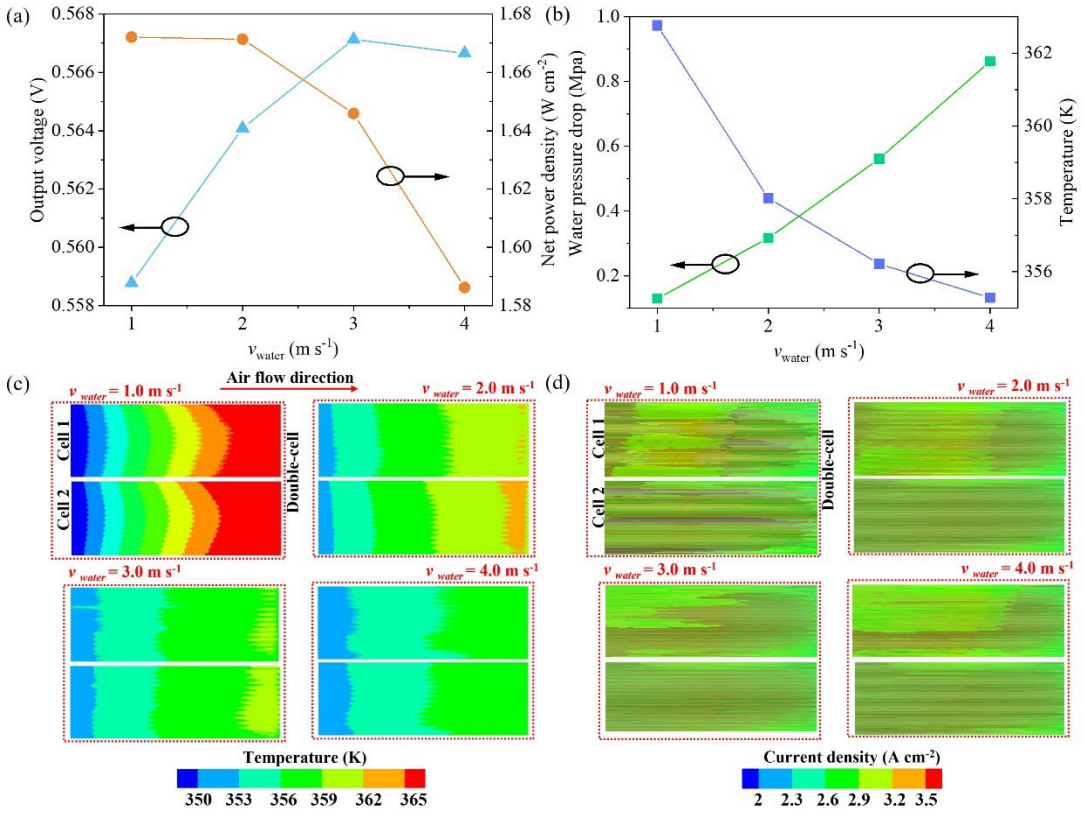

Figure 4. Effect of velocity of cooling water on (a) Output voltage and net power density; (b) Water pressure drop of cooling channel and temperature in the middle plane of the cathode CL; (c) Temperature distribution in the middle plane of the cathode CL; (d) Current density distribution in the middle plane of the membrane of double-cell structure.